Published in final edited form as:
J Allergy Clin Immunol. 2013 April ; 131(4): 1157–1166. doi:10.1016/j.jaci.2013.01.008.

The Proteome of TLR3-stimulated human immortalized fibroblasts; implications for susceptibility to herpes simplex encephalitis

Rebeca Pérez de Diego, PhD[1,2,3,4,*], **Claire Mulvey, PhD**[5,6], **Mark Crawford, BSc**[5], **Matthew W.B. Trotter, PhD**[7], **Lazaro Lorenzo, BSc**[1,2,3], **Vanessa Sancho-Shimizu, PhD**[1,2,3], **Laurent Abel, MD, PhD**[1,2,3], **Shen-Ying Zhang, MD, PhD**[1,2,3], **Jean-Laurent Casanova, MD, PhD**[1,2,3,8,9], and **Jasminka Godovac-Zimmermann, PhD**[5]

[1]Laboratory of Human Genetics of Infectious Diseases, Necker Branch, INSERM U980, Necker Medical School, Paris 75015, France, EU

[2]University Paris Descartes, Paris 75015, France, EU

[3]St. Giles Laboratory of Human Genetics of Infectious Diseases, Rockefeller Branch, The Rockefeller University, New York, NY 10065, USA

[4]Immunology Unit, IdiPAZ Institute for Health Research, La Paz University Hospital, 261 Pº Castellana, Madrid 28046, Spain, EU

[5]Division of Medicine, University College London, 5 University Street, London WC1E 6JF, UK, EU

[7]The Anne McLaren Laboratory for Regenerative Medicine and Department of Surgery, University of Cambridge, Cambridge CB2 0SZ, UK, EU. Present Address: Celgene Institute Translational Research Europe, Parque Científico y Tecnológico Cartuja 93, Seville 41092, Spain, EU

[8]Prince NaifCenter for Immunology Research, Department of Pediatrics, College of Medicine, King Saud University, Riyadh 11451, Saudi Arabia

[9]Pediatric Hematology-Immunology Unit, Necker Hospital, Paris 75015, France, EU

Abstract

Background—Inborn errors in the Toll like receptor 3 (TLR3)-Interferon (IFN) type I and III pathway have been implicated in susceptibility to herpes simplex virus encephalitis (HSE) in children, but most patients studied do not carry mutations in any of the genes presently associated with HSE-susceptibility. Moreover, many patients do not display any TLR3-related fibroblastic phenotype.

[*]**Corresponding author:** Rebeca Perez de Diego, Address;Immunology Unit, IdiPAZ Institute for Health Research, La Paz University, Hospital, 261 Pº Castellana, Madrid 28046, Spain, EU, Telephone: 0034 91 727 7238, Fax: 0034 91 727 7095, rebeca.perez@idipaz.es / perezdediegor@gmail.com.
[6]Present Address: Cambridge Centre for Proteomics, Cambridge Systems Biology Centre, Department of Biochemistry, University of Cambridge, Tennis Court Road, CB2 1QR, Cambridge, UK, EU.

Since initial involvement in the work, M.W.B.T. has become an employee of Celgene Research SLU, part of Celgene Corporation, and declares no conflicts of interest.

Objective—This suggests the study of other signalling pathways downstream of TLR3 and/or other independent pathways which may contribute to HSE susceptibility.

Methods—We have used the stable isotope labelling of amino acids in cell culture (SILAC) proteomics methodology to measure changes in the human immortalized fibroblast proteome after TLR3 activation.

Results—Cells from healthy controls were compared to cells from a patient with a known genetic aetiology of HSE (UNC93B$^{-/-}$) and also to cells from an HSE patient with an unknown gene defect. Consistent with known variation in susceptibility of individuals to viral infections, substantial variation in the response level of different healthy controls was observed, but common functional networks could be identified, including upregulation of superoxide dismutase 2 (SOD2). The HSE patients show clear differences in functional response networks when compared to healthy patients and also when compared to each other.

Conclusions—The present study delineates a number of novel proteins, TLR3-related pathways and cellular phenotypes that may help elucidate the genetic basis of childhood HSE. Furthermore, our results reveal SOD2 as a potential therapeutic target for amelioration of the neurological sequelae caused by HSE.

Keywords

Herpes simplex encephalitis (HSE); SILAC; proteomics; mass spectrometry; fibroblast; herpes simplex virus 1 (HSV-1); TLR3; interferon (IFN)

INTRODUCTION

Herpes simplex virus (HSV-1) encephalitis (HSE) is a devastating infection of the central nervous system (CNS)[1]. HSE is the most common form of sporadic viral encephalitis in Western countries, where it is estimated to occur in approximately 1 in 250,000 individuals per year. It peaks in childhood between the ages of 3 months and 6 years during primary infection with HSV-1, which reaches the CNS via a neurotropic route involving the trigeminal and olfactory nerves[2, 3]. Treatment with acyclovir decreases the mortality rate in affected children, but significant neurological impairment is observed in most survivors, young children in particular. HSV-1 is widespread and typically innocuous in human populations. Childhood HSE has not been associable with known immunodeficiencies and its pathogenesis remained elusive until we identified the first three genetic etiologies of this condition[4, 5]. Autosomal recessive UNC-93B deficiency abolishes Toll-like receptor (TLR) 3,7,8, and 9 signaling[6], whereas autosomal dominant TLR3 deficiency specifically affects TLR3 signaling[7]. Recently an autosomal dominant deficiency in TNF receptor-associated factor 3 (TRAF3), an adaptor molecule implicated in the TLR3 pathway, and Toll/IL1R (TIR) domain-containing adaptor inducing IFN-β (TRIF) deficient patients has been described[8, 9]. These studies suggested that childhood HSE may result from impaired interferon (IFN)-α/β and IFN-λ production in response to the stimulation of TLR3 by dsRNA intermediates of HSV-1 in the CNS. However, only a small fraction of children with HSE carry mutations in *UNC93B1, TLR3, TRIF* or *TRAF3*. The study of proteins implicated in the TLR3-IFN pathway for HSE patients enrolled in our laboratory (226 patients) has revealed that only a small proportion of patients bear a genetic defect in these proteins. A larger proportion of patients display an impaired production of IFN type I and III upon TLR3 stimulation of their fibroblasts. Other patients do not show the fibroblastic phenotype associated with impaired IFN production; in these patients the gene defect may affect other pathway(s) that are normally activated in fibroblasts after TLR3 stimulation. In the present study, as an approach to define new candidate genes for HSE, we have used

proteomics methods to characterize TLR3-dependent pathways in fibroblasts that might be correlated with HSV-1 infection in the CNS.

METHODS

Subjects and patient P case report

The experimental protocol was approved by the Ethical Committee of Necker-Enfants Malades Hospital (Paris, France) and written informed consent was obtained for this study. P is a French boy of non-consanguineous descent with no family history of encephalitis. At the age of eight years, he suffered fever, convulsions and hemiparesis and he was diagnosed with HSE.

Cell purification

Primary human fibroblasts were obtained from biopsies of an UNC-93B-deficient patient[6], three healthy controls, and one HSE patient with unknown gene defect. They were then transformed with an SV-40 vector, as previously described[10], to create immortalized fibroblast cell lines: SV40-fibroblasts.

Stable isotope labelling with amino acids in cell culture (SILAC) labelling of human SV40-fibroblast

Cells were grown for six rounds of cell division in DMEM containing 13C6, 15N4 L-arginine, 13C6 L-lysine (Invitrogen, Carlsbad, California, USA) (heavy medium) supplemented with 10% dialysed FCS (Invitrogen) to ensure all the cellular proteins were labelled to saturation. The SILAC technique relies on the intrinsic metabolic machinery of the cell to incorporate “heavy” amino acids into all newly synthesized proteins. Immortalized fibroblast cell lines were used to achieve the full SILAC incorporation without detrimentally affecting the characteristics of the cell line. Our previous work has demonstrated that SV40 immortalised fibroblasts can successfully be used to study TLR3 signalling[7–9].

Labelled cells were activated in 24-well plates, at a density of 10^5 cells/well, with 25 μg/ml polyinosinepolycytidylic acid (poly(I:C)), a TLR3 agonist (InvivoGen, San Diego, CA, USA), for 24 hours. Unlabelled cells were grown in parallel in medium containing normal amino acids (light medium) and were not stimulated. The SILAC labels were shown to be fully incorporated before the experiment was conducted (data not shown).

Protein Separation and In-Gel Enzymatic Digestion

Equal amounts of protein from unlabelled “light” (non-stimulated) and labelled “heavy” (stimulated) cells were mixed and subsequently separated by SDS-PAGE (BioRad Laboratories, Hercules, CA, USA). Proteins were visualized by silver-staining (Sigma, St Louis, MO, USA) and the gel lane was divided into approximately 34 equally sized pieces which were excised from the gel and destained (30mM $K_3Fe(CN)_6$; 100mM $Na_2S_2O_3$) prior to further processing. Gel processing was conducted with a Progest Investigator Instrument (DigiLab, Genomics Solutions, Cambs, UK) for reduction and alkylation according to established protocols[11]. Briefly, the gel pieces were washed with three cycles of 25 mM NH_4HCO_3 pH 8.0 and acetonitrile. Finally, gel plugs were rehydrated in 20 μg/mL sequencing grade modified trypsin (Promega, Hamps, UK) and incubated overnight at 37C. Tryptic peptides were eluted, vacuum-dried, and resuspended in 0.1% formic acid.

XCalibur raw files were processed by Quant.exe and Identify.exe of the MaxQuant suite (version 1.0.13.13), in combination with the Mascot search engine (version 2.2, Matrix Science, U.K.), and searched against a concatenated International Protein Index (IPI) human

protein database(version 3.54; containing 75,710 entries, including 262 commonly observed contaminants such as porcine trypsin and some human keratins). All proteins were filtered according to a false discovery rate (FDR) of 1% applied at both peptide and protein levels. Proteins were automatically quantified in the MaxQuant software. In the final results files, all Protein Groups with a normalized ratio SigB score of ≤0.05 and a normalised ratio > 1.5 were accepted for downstream analysis. Experiments were done induplicate and all proteins discussed in the text were significant in both replicates for each sample. For details of mass spectrometry analysis, protein inference and quantification, analysis of sample correlations and global functional analysis of protein networks, see Additional Methods at the Online Repository.

Transient transfections

SV40-fibroblasts were transfected with 2 μg of pBI-EGFP-MnSOD (SOD2) or pTRE-Tight-BI-AcGFP1 (Clontech, Palo Alto, CA, USA) as mock vector, in the presence of the FuGENE ®HD Transfection Reagent (Roche Applied Science, Indianapolis, IN, USA), according to manufacturer's instructions. 24 hours post-transfection, SV40-fibroblasts were activated by incubation with 25 μg/ml poly(I:C) (InvivoGen) for 24 h. pTRE-Tight-BI-AcGFP1 was used as mock vector (pBI-EGFP has been replaced by AcGFP; it has 94% identical amino acid sequence and same biophysical properties).

Western blot

Total cell extracts were prepared from SV40-fibroblasts, both transfected and not transfected. Equal amounts of protein from each sample were separated by SDS-PAGE and blotted onto iBlot™ Gel Transfer Stacks (Invitrogen). Membranes were probed with anti-ICAM-1 rabbit monoclonal (Lifespan Biosciences, Seattle, WA, USA), anti-SOD2 and ITGA2 monoclonals and anti-ITGA5 and PPIF polyclonals (Abcam, Cambridge, MA, USA), anti-ANXA5/7 monoclonals (SantaCruz Biotechnology Inc., SantaCruz, CA), followed by a secondary anti-mouse or rabbit IgG (GEHealthcare, Buckinghamshire, UK). Membranes were stripped and reprobed with anti-GADPH (SantaCruz) to control for protein loading. Antibody binding was detected by enhanced chemiluminescence (ECL; Amersham-Pharmacia-Biotech).

Apoptosis analysis

Levels of SV40-fibroblast apoptosis after poly(I:C) stimulation were assessed by measures of caspase-3 and 7 activity. Cells were plated, in triplicate, in Microtest™ 96 well Assay Plate, Optilux™ Black/Clear Bottom (Falcon, Becton Dickinson, Franklin Lakes, NJ, USA) (1×10^4 cells/well), in DMEM supplemented with 2% FCS; some cells were transfected with 150 ng per well of pBI-EGFP-MnSOD (SOD2) or pTRE-Tight-BI-AcGFP1 as mock vector. 24 hours later, cells were treated with poly(I:C) (25 μg/ml) and incubated for 24h. Caspase-3 and 7 activity was measured 48 hours post-transfection by Caspase-Glo® 3/7 Assay (Promega) as per manufacturer's instructions.

IFN type I and III determination

SV40-fibroblast cell lines were activated in 24-well plates at a density of 10^5 cells/well and stimulated with poly(I:C) at a concentration of 25 μg/ml for 24 h. Cells were grown at 37°C under an atmosphere containing 5% CO_2. Cell supernatants were recovered and an ELISA was performed for IFN-β (TFB, Fujirebio, Inc., Tokyo, Japan) according to manufacturer's instructions. The ELISA for IFN-λ was performed as previously described[7].

RESULTS

Identification of proteins up-regulated in human SV40 fibroblasts following TLR3 activation

Response to TLR3 activation was defined by altered levels of protein abundance in human SV40-fibroblasts when stimulated with poly(I:C) (used as TLR3 agonist[6–9]) and was measured by SILAC/MS[12–14] monitoring of heavy/light isotope labelling ratios for peptides from proteins of stimulated/unstimulated cells (Figure 1A).

Three Healthy samples (C1, C2 and C3) are positive controls that provide a measure of variability between individuals (Figure 1B). Negative control, C2NS, is a healthy sample with strong TLR3 response, but for which neither cell population (light/heavy) was stimulated (Figure 1B). The UNC-93B-deficiency blocks TLR3, 7, 8 and 9 pathways, so cells from the UNC-93B$^{-/-}$ patient (sample UNC-93B$^{-/-}$) should not respond to TLR3 agonists[6]. We used SV40-fibroblasts from a homozygous UNC-93B$^{-/-}$ patient rather than a patient with heterozygous TLR3 mutation due to the complete deficiency of TLR3 pathways observed in UNC93B$^{-/-}$ cells[6]. Finally, we included cells from an HSE patient with unknown gene defect (P) (Figure 1B), which produce detectable amounts of IFN type I after TLR3 stimulation (Figure 2).

All six biological samples were subjected to duplicate MS analysis[15, 16] and protein lists were obtained by combining both datasets prior to analysis of differential protein abundance (E Table 1–6). The MS data is summarized in Figure 1C, and E Figure 1 illustrates the quality of the MS data for a single SILAC peptide pair detected in a key protein of our study.

Figure 1C shows the number of proteins found to be significantly upregulated (normalized H/L (SILAC) ratio ≥ 1.5 and Significance B (SigB)[16] < 0.05, see below) in the different cells following activation (except for C2NS) with poly(I:C). We have previously observed variability in response of healthy control fibroblasts upon TLR3 stimulation, particularly in terms of cytokine and interferon production (Figure 2). To take this into account, we included sample C3, from a healthy donor with known weaker response to TLR3 stimulation compared to C1 and C2 (Figure 2). In line with expectation, this control showed a reduced number of upregulated proteins (19 with SILAC H/L ratios between 1.50-fold and 2.15-fold; Figure 1C). Comparison of upregulated proteins between the control samples revealed variation in those proteins most strongly upregulated. This variability might arise from a) the conservative condition that protein SILAC ratios were calculated from at least three separate H/L ratio measurements, and/or b) differences in the extent to which different proteins change in abundance in cells taken from different individuals. A qualitative test of cellular variability amongst healthy controls displays biologically-relevant positive correlation distinguishable from the negative control (C2NS) (see Additional Results, E Figure 2, E Figure 3 and E Table 7 at the Online Repository).

Detection of Functional Networks

Given the observed variability in detection and measurement of specific protein regulation across experiments, we sought common functional networks amongst the most strongly upregulated proteins in order to characterise response to TLR3 stimulation and identify disease-related differences by comparison. We used MetaCore™ version 6.3 (GeneGo Inc.) to investigate pathways and biological functions represented by differentially regulated proteins in all samples (see Additional Results and E Figure 2 at the Online Repository).

The analysis indicated that the most significant GeneGo process networks for C1/C2/C3 are similar and are implicated in immune responses, such as IFN-signalling and antigen

presentation pathways (Table 1A), known to be implicated following TLR3 stimulation[17, 18]. Similar analysis was performed for the non-stimulated C2NS control sample. The majority of proteins in the non-stimulated control C2NS show SILAC ratios ≈ 1 (E Table 4) which represent "measurement noise". As may be expected, the 8 proteins designated as upregulated (H/L = 1.50 to 3.07-fold) did not associate with canonical pathways or process networks implicated in immune response, and networks inferred from them were of limited statistical significance and scattered over diverse pathways and processes (Table 2A). The UNC-93B$^{-/-}$ sample did not associate with the immune-related networks identified above, further suggesting that the TLR3 pathway is completely abolished by this deficiency (Table 2B). UNC-93B$^{-/-}$ did, however, yield several upregulated proteins (E Table 5), with SILAC ratios of 1.5 to 3.95-fold, which may represent attempts by these cells to compensate for the genetic defect. Canonical pathways associated with these proteins were largely metabolic (glycolysis, gluconeogenesis, fructose metabolism), however, and process networks inferred were particularly diverse (Table 2B).

The same analysis was also performed on the union of proteins upregulated in C1/C2/C3 (152 proteins, excluding 7 proteins in common withC2NS or UNC-93B$^{-/-}$ samples), strengthening the association between TLR3 stimulation and IFN α/β signalling pathways (Table 1B, E Figure 4) and further suggesting a clear proteomic signature for activation of these pathways upon TLR3 stimulation.

The analysis of healthy controls also revealed other statistically significant proteins/pathways/processes (Table 1B) that do not appear in similar analysis of C2NS or UNC-93B$^{-/-}$ samples (Table 2), and which have not been associated previously with TLR3 pathways. Such proteins included Intercellular adhesion molecule-1 (ICAM-1), integrins ITGA2 and 5, and Superoxide dismutase 2 (SOD2) (Table 1B). Furthermore, some proteins upregulated by TLR3 stimulation in healthy controls were not placed in pathways/networks by GeneGo, but are associated with a role in HSV infection in the CNS by literature evidence. These proteins include several Annexins and Peptidyl-propyl cis-trans isomerise mitochondrial (PPIF) (E Table 1–3), the majority of which were not identity as differentially regulated by analysis of UNC-93B$^{-/-}$ (Figure 3A). E Table 8 shows MS data for individual peptides assigned to these proteins and confirms the quality of their detection and assignment. The expression of these proteins was confirmed by western blot (WB) (E Figure 5) and they are considered further in the discussion.

Finally, although not the primary focus of our analysis, the union of proteins commonly downregulated upon TLR3 stimulation in healthy controls C1/C2/C3 were subjected to similar pathway analysis. The results are summarised in E Tables 1–3 and reflect strongest association with cytoskeleton remodelling and negative regulation of cell cycle, in accordance with the apoptosis induced upon TLR3 stimulation and in agreement, for example, with upregulation of annexins identified above.

Proteomics of TLR3 stimulated fibroblasts reveals potential new treatments for HSE: SOD2 upregulation

SOD2 is highly upregulated in healthy patient samples C1, C2 and C3 after TLR3 stimulation but not in cells from a patient with known genetic deficiency UNC-93B$^{-/-}$ and neither in unstimulated healthy control sample C2NS (Figure 3A). SOD2 is an antioxidant enzyme strongly upregulated after TLR3 activation in macrophages, protecting these cells from oxidative stress during microbial infection[19]. SOD2 is increased after HSV-1 infection and SOD2 levels in the CNS are associated with neuronal protection[20, 21]. Other examples of the protective role of SOD2 have been shown in an animal model of complex I deficiency[22], in which SOD2 gene transfer *in vivo* enhanced cellular resistance to reactive oxygen species and suppressed degeneration of the optic nerve[22]. This suggests SOD2 as a

putative target for future treatment of HSE, in particular to reduce the neurological sequelae that patients suffer after encephalitis.

We used gene transfer to further investigate the role of SOD2 in human transformed fibroblasts. WB of healthy cells confirmed upregulation of SOD2 after poly(I:C) stimulation, and very low levels of SOD2 in UNC-93B$^{-/-}$ cells suggested that the defect affects SOD2 expression (Figure 4A). We detected SOD2 overexpression after transient transfections of pBI-EGFP-MnSOD (SOD2), but not with mock transfected vector (Figure 4A). Measurement of apoptosis in SV40-fibroblasts transfected with SOD2 showed that healthy cells overexpressing SOD2 are protected against apoptosis and that this is also the case for stimulation with poly(I:C). Relative apoptosis measured in poly(I:C) stimulated UNC-93B$^{-/-}$ cells against their non-stimulated counterpart was higher than similar measurement for healthy controls, indicating UNC-93B$^{-/-}$ patient cells as more susceptible to apoptosis than healthy cells after TLR3 activation. When transfected with SOD2, however, UNC-93B$^{-/-}$ patient cells were protected against apoptosis (Figure 4B). Together, these results suggest that pharmacological agents that upregulate SOD2 expression or activity could exert a protective anti-oxidant response mechanism to reduce the cell death associated with TLR3 stimulation in HSE patients.

Analysis of a patient with unknown gene defect and without fibroblastic phenotype

30% of HSE patients analyzed do not show the fibroblastic phenotype characterized by reduced IFN type I and III production after TLR3 stimulation (data not shown). In these patients, study of the TLR3 stimulated proteome may help delineate the source(s) of the different cellular phenotype. We conducted a SILAC analysis of a patient whose genetic defect is unknown, but which produces significant amounts of IFN type I and III after TLR3 stimulation (E Figure 6A). The study identified many upregulated proteins shared with stimulated healthy control samples C1, C2 and C3, and which were not observed for UNC93B$^{-/-}$. The proteins shared those highlighted during earlier analysis of the stimulated healthy controls; with the exception of ICAM-1, which was not detected post-stimulation (Figure 3A and E Table 6) as confirmed by WB analysis (E Figure 6B). ITGA5 (H/L = 1.65) and ANX 11 (H/L = 1.29) are upregulated in patient sample P, but at a ratio significance just outside the threshold of SigB < 0.05 (E Table 6). GeneGo analysis also inferred process networks similar to those related to stimulation of healthy controls, involving immune responses such as IFN-signalling and antigen presentation pathways (Table 2C). This result concurs with previous studies that show cells from patient P to exhibit IFN type I and III production after TLR3 signalling (E Figure 6A). Given the extent of overlap between the analysis of TLR3 stimulation effect in patient P and that in healthy control samples, the non-detectable levels of ICAM-1 upon TLR3 stimulation in P, identified via proteomic analysis, provide an avenue in this patient for a candidate approach centred on ICAM-1 and related genes/proteins. This would be the first such approach in an HSE patient to involve pathways beyond TLR3-IFN signalling.

DISCUSSION

The quantitative SILAC analysis presented here provides important preliminary evidence to suggest that several proteins, pathways and processes could play important and novel roles in TLR3 response and HSE immunity.

ICAM-1 upregulation

After TLR3 stimulation, healthy controls C1, C2 and C3 displayed ICAM-1 upregulation, as described previously[23, 24], but there was no corresponding upregulation in UNC-93B$^{-/-}$, patient P or non-stimulated C2NS (Figure 3A and E Figure 6). ICAM-1 is an intercellular

adhesion molecule implicated in HSV-1 infection in CNS[25, 26]. The present results suggest that lack of ICAM upregulation may be an important factor in susceptibility to HSE, especially for those patients (e.g. P) which show substantial IFN production and lack the fibroblastic phenotype.

Upregulation of integrins ITGA2 and ITGA5

We detected ITGA2 and 5 upregulation after TLR3 stimulation in healthy cells but not in C2NS or UNC-93B$^{-/-}$ (Figure 3A). Cells from patient P showed significant upregulation of ITGA2 (Figure 3A) and upregulation of ITGA5 (H/L = 1.65) just beyond the significance threshold employed (E Table 6). Some studies have demonstrated that integrins are necessary for HSV-1 entry/fusion in cells[27] and ITGA2 is upregulated in chronic hepatitis virus infection[28]. The present results identify specific integrins upregulated following TLR3 activation and whose further investigation might offer new insights into HSE susceptibility.

Upregulation of Annexins

After TLR3 stimulation in healthy cells, we detected upregulation of several annexins (Figure 3A). Microglial cells, after activation in response to harmful stimuli, are able to induce neuronal cell death by ANX1[29] and ANX5 upregulation[30]. It has been shown that TLR3 activation with poly(I:C) and HSV-1 infection induce apoptosis by enhancing ANX5 levels[31–33]. The present data suggests possible roles for ANX5, 6, 7 in the activation and subsequent apoptosis of immune cells in the CNS upon viral infection.

PPIF upregulation

PPIF protein was upregulated after TLR3 stimulation in healthy and patient P cells, but not in those with UNC-93B$^{-/-}$ defect (Figure 3A). PPIF, also called Cyclophilin D, is part of the mitochondrial permeability transition pore in the inner mitochondrial membrane. Activation of this pore is thought to be involved in the induction of apoptotic and necrotic cell death. HSV-1 infection of neurons is known to induce cell death and PPIF has been previously described as a key protein in neuronal cell death[34–36]. This is the first report of a relationship between PPIF and TLR3, suggesting a possible role for PPIF in HSE immunity.

Previous studies have shown that the TLR3 pathway is essential for susceptibility to HSE[6–8]. However the analysis of many proteins downstream of TLR3 implicated in the TLR3-IFN type I pathway has failed to reveal a genetic defect in most patients analyzed. In 226 patients enrolled in our laboratory, we have detected mutations in *UNC93B1, TLR3* or genes downstream of the TLR3 pathway in a very low percentage. Conversely, study of IFN type I and III production after TLR3 activation in SV40-fibroblasts of HSE patients has shown that only 30%, of a total of 89 patients analyzed, have normal IFN type I and III production (data not shown). This suggests that despite the importance of the TLR3 pathway in HSE immunity, genetic defect(s) responsible for susceptibility to HSV-1 in the CNS could be due to TLR3-independent pathways, or other TLR3, IFN-dependent pathways that are activated after initial TLR3 activation. Overall, the present results suggest a rich diversity of pathways downstream of TLR3 activation that may be relevant for HSE susceptibility and which invite further investigation.

Proteomic analysis of a patient (P) with unknown gene defect but without the fibroblastic phenotype has revealed a lack of ICAM-1, delineating a cellular phenotype which may assist dissection of this genetic aetiology. Finally, an important problem in this pathology is post-infection neurological sequelae, for which the current treatment is aciclovir, an antiviral drug. However, this treatment is largely uneffective[2]. The present study has now revealed SOD2 as a possible therapeutic target for prevention of the neurological sequelae suffered by HSE patients.

Proteomics has reached the stage where its methods are well developed and capable of generating large, robustly identified, high resolution quantitative datasets that provide a wealth of knowledge at the systems level. Even for a disease such as HSE, of apparent aetiological diversity, coupled with the cellular diversity evident amongst individuals, proteomics has provided an integrated overview of cellular responses that may be crucial for understanding the dynamics of HSE susceptibility.

Supplementary Material

Refer to Web version on PubMed Central for supplementary material.

Acknowledgments

We thank the members of the Laboratory of Human Genetics of Infectious Diseases, especially Marjorie Hubeau, Dr C. Guerrera and Prof. L.R. Brown for helpful advice. We thank Mariana Díaz Almiron (Biostatistical Unit, IdiPaz-Hospital La Paz) for the biostatistical analysis. We thank the patient and her family for their participation in this study, which was supported by the AXA Research Fund, the *Groupement d'Intérêt Scientifique Maladies Rares*, the *Action Concertée Incitative de Microbiologie*, the March of Dimes, the *Agence Nationale pour la Recherche*, the Eppley Foundation, the National Institute of Allergy and Infectious Diseases grant number R01AI088364, the Thrasher Research Fund, the Jeffrey Modell Foundation, Talecris Biotherapeutics, the St. Giles Foundation, the National Center for Advancing Translational Sciences (NCATS) of the National Institutes of Health (NIH) grant number 8UL1TR000043, and the Rockefeller University. P.R. is supported by a European Union FP6 grant. J.-L.C. was an international scholar of the Howard Hughes Medical Institute until 2008. The work was supported by The Wellcome Trust Grant to J. G-Z.

Abbreviations

HSE	Herpes simplex virus encephalitis
SILAC	Stable isotope labelling of amino acids in cell culture
HSV-1	Herpes simplex virus
CNS	Central nervous system
TLR	Toll-like receptor
TRAF3	TNF receptor-associated factor 3
TRIF	Toll/IL1R (TIR) domain-containing adaptor inducing IFN-β
IFN	Interferon
poly(I:C)	Polyinosinepolycytidylic acid
SigB	Significance B
ICAM-1	Intercellular adhesion molecule-1
SOD2	Superoxide dismutase 2
PPIF	Peptidyl-propyl cis-trans isomerise mitochondrial
MS	Mass Spectrometry

REFERENCES

1. Whitley RJ. Herpes simplex encephalitis: adolescents and adults. Antiviral Res. 2006; 71:141–148. [PubMed: 16675036]
2. De Tiege X, Rozenberg F, Heron B. The spectrum of herpes simplex encephalitis in children. Eur J Paediatr Neurol. 2008; 12:72–81. [PubMed: 17870623]

3. Abel L, Plancoulaine S, Jouanguy E, Zhang SY, Mahfoufi N, Nicolas N, et al. Age-Dependent Mendelian Predisposition to Herpes Simplex Virus Type 1 Encephalitis in Childhood. J Pediatr. 2010
4. Casanova JL, Abel L. Primary immunodeficiencies: a field in its infancy. Science. 2007; 317:617–619. [PubMed: 17673650]
5. Alcais A, Abel L, Casanova JL. Human genetics of infectious diseases: between proof of principle and paradigm. J Clin Invest. 2009; 119:2506–2514. [PubMed: 19729848]
6. Casrouge A, Zhang SY, Eidenschenk C, Jouanguy E, Puel A, Yang K, et al. Herpes simplex virus encephalitis in human UNC-93B deficiency. Science. 2006; 314:308–312. [PubMed: 16973841]
7. Zhang SY, Jouanguy E, Ugolini S, Smahi A, Elain G, Romero P, et al. TLR3 deficiency in patients with herpes simplex encephalitis. Science. 2007; 317:1522–1527. [PubMed: 17872438]
8. Perez de Diego R, Sancho-Shimizu V, Lorenzo L, Puel A, Plancoulaine S, Picard C, et al. Human TRAF3 adaptor molecule deficiency leads to impaired Toll-like receptor-3 response and susceptibility to herpes simplex encephalitis. Immunity. 2010; 33:400–411. [PubMed: 20832341]
9. Sancho-Shimizu V, Perez de Diego R, Lorenzo L, Halwani R, Alangari A, Israelsson E, et al. Herpes simplex encephalitis in children with autosomal recessive and dominant TRIF deficiency. J Clin Invest. 2011; 121:4889–4902. [PubMed: 22105173]
10. Chapgier A, Wynn RF, Jouanguy E, Filipe-Santos O, Zhang S, Feinberg J, et al. Human complete Stat-1 deficiency is associated with defective type I and II IFN responses in vitro but immunity to some low virulence viruses in vivo. J Immunol. 2006; 176:5078–5083. [PubMed: 16585605]
11. Shevchenko A, Wilm M, Vorm O, Mann M. Mass spectrometric sequencing of proteins silver-stained polyacrylamide gels. Anal Chem. 1996; 68:850–858. [PubMed: 8779443]
12. Ong SE, Blagoev B, Kratchmarova I, Kristensen DB, Steen H, Pandey A, et al. Stable isotope labeling by amino acids in cell culture, SILAC, as a simple and accurate approach to expression proteomics. Mol Cell Proteomics. 2002; 1:376–386. [PubMed: 12118079]
13. Ong SE, Foster LJ, Mann M. Mass spectrometric-based approaches in quantitative proteomics. Methods. 2003; 29:124–130. [PubMed: 12606218]
14. Mulvey C, Tudzarova S, Crawford M, Williams GH, Stoeber K, Godovac-Zimmermann J. Quantitative proteomics reveals a "poised quiescence" cellular state after triggering the DNA replication origin activation checkpoint. J Proteome Res. 2010; 9:5445–5460. [PubMed: 20707412]
15. Cox J, Mann M. MaxQuant enables high peptide identification rates, individualized p.p.b.-range mass accuracies and proteome-wide protein quantification. Nat Biotechnol. 2008; 26:1367–1372. [PubMed: 19029910]
16. Cox J, Matic I, Hilger M, Nagaraj N, Selbach M, Olsen JV, et al. A practical guide to the MaxQuant computational platform for SILAC-based quantitative proteomics. Nat Protoc. 2009; 4:698–705. [PubMed: 19373234]
17. Matsumoto M, Seya T. TLR3: interferon induction by double-stranded RNA including poly(I:C). Adv Drug Deliv Rev. 2008; 60:805–812. [PubMed: 18262679]
18. Uematsu S, Akira S. Toll-like receptors and Type I interferons. J Biol Chem. 2007; 282:15319–15323. [PubMed: 17395581]
19. Rakkola R, Matikainen S, Nyman TA. Proteome analysis of human macrophages reveals the upregulation of manganese-containing superoxide dismutase after toll-like receptor activation. Proteomics. 2007; 7:378–384. [PubMed: 17211829]
20. Hill JM, Lukiw WJ, Gebhardt BM, Higaki S, Loutsch JM, Myles ME, et al. Gene expression analyzed by microarrays in HSV-1 latent mouse trigeminal ganglion following heat stress. Virus Genes. 2001; 23:273–280. [PubMed: 11778695]
21. Saha RN, Pahan K. Differential regulation of Mn-superoxide dismutase in neurons and astroglia by HIV-1 gp120: Implications for HIV-associated dementia. Free Radic Biol Med. 2007; 42:1866–1878. [PubMed: 17512466]
22. Qi X, Lewin AS, Sun L, Hauswirth WW, Guy J. SOD2 gene transfer protects against optic neuropathy induced by deficiency of complex I. Ann Neurol. 2004; 56:182–191. [PubMed: 15293270]

23. Rydberg C, Mansson A, Uddman R, Riesbeck K, Cardell LO. Toll-like receptor agonists induce inflammation and cell death in a model of head and neck squamous cell carcinomas. Immunology. 2009; 128:e600–e611. [PubMed: 19740321]
24. Starace D, Galli R, Paone A, De Cesaris P, Filippini A, Ziparo E, et al. Toll-like receptor 3 activation induces antiviral immune responses in mouse sertoli cells. Biol Reprod. 2008; 79:766–775. [PubMed: 18596219]
25. Brankin B, Hart MN, Cosby SL, Fabry Z, Allen IV. Adhesion molecule expression and lymphocyte adhesion to cerebral endothelium: effects of measles virus and herpes simplex 1 virus. J Neuroimmunol. 1995; 56:1–8. [PubMed: 7822475]
26. Noisakran S, Harle P, Carr DJ. ICAM-1 is required for resistance to herpes simplex virus type 1 but not interferon-alpha1 transgene efficacy. Virology. 2001; 283:69–77. [PubMed: 11312663]
27. Parry C, Bell S, Minson T, Browne H. Herpes simplex virus type 1 glycoprotein H binds to alphavbeta3 integrins. J Gen Virol. 2005; 86:7–10. [PubMed: 15604426]
28. Bieche I, Asselah T, Laurendeau I, Vidaud D, Degot C, Paradis V, et al. Molecular profiling of early stage liver fibrosis in patients with chronic hepatitis C virus infection. Virology. 2005; 332:130–144. [PubMed: 15661146]
29. Parente L, Solito E. Annexin 1: more than an anti-phospholipase protein. Inflamm Res. 2004; 53:125–132. [PubMed: 15060718]
30. Li L, Lu J, Tay SS, Moochhala SM, He BP. The function of microglia, either neuroprotection or neurotoxicity, is determined by the equilibrium among factors released from activated microglia in vitro. Brain Res. 2007; 1159:8–17. [PubMed: 17572395]
31. Jiang Q, Wei H, Tian Z. Poly I:C enhances cycloheximide-induced apoptosis of tumor cells through TLR3 pathway. BMC Cancer. 2008; 8:12. [PubMed: 18199340]
32. Gillis PA, Okagaki LH, Rice SA. Herpes simplex virus type 1 ICP27 induces p38 mitogen-activated protein kinase signaling and apoptosis in HeLa cells. J Virol. 2009; 83:1767–1777. [PubMed: 19073744]
33. Swarup V, Ghosh J, Duseja R, Ghosh S, Basu A. Japanese encephalitis virus infection decrease endogenous IL-10 production: correlation with microglial activation and neuronal death. Neurosci Lett. 2007; 420:144–149. [PubMed: 17531383]
34. Baines CP, Kaiser RA, Purcell NH, Blair NS, Osinska H, Hambleton MA, et al. Loss of cyclophilin D reveals a critical role for mitochondrial permeability transition in cell death. Nature. 2005; 434:658–662. [PubMed: 15800627]
35. Li V, Brustovetsky T, Brustovetsky N. Role of cyclophilin D-dependent mitochondrial permeability transition in glutamate-induced calcium deregulation and excitotoxic neuronal death. Exp Neurol. 2009; 218:171–182. [PubMed: 19236863]
36. Du H, Guo L, Fang F, Chen D, Sosunov AA, McKhann GM, et al. Cyclophilin D deficiency attenuates mitochondrial and neuronal perturbation and ameliorates learning and memory in Alzheimer's disease. Nat Med. 2008; 14:1097–1105. [PubMed: 18806802]

CLINICAL IMPLICATIONS

Quantitative SILAC-based proteome analysis of TLR3-stimutated human immortalized fibroblasts can delineate cellular phenotypes and may be used to dissect the genetic basis of childhood herpes simplex encephalitis (HSE), as well as new potential therapeutics targets.

A

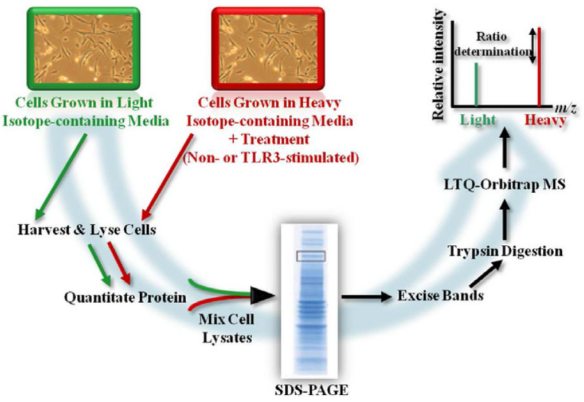

B

	TLR3 stimulation with Poly(I:C)	TLR3 pathway in genetic terms	**Final activation state for TLR3**
C1, C2 and C3	Yes	WT (healthy donor-1, 2 and 3 respectively)	**Activated**
C2NS	No	WT (healthy donor-2)	**Not activated due to non-stimulation**
UNC-93B$^{-/-}$	Yes	Blocked due to UNC93B deficiency (HSE patient)	**Not activated due to genetic defect**
P	Yes	Unknown gene defect (HSE patient)	**Unknown**

C

	C1	**C2**	**C3**	**C2NS**	**UNC-93B$^{-/-}$**	**P**
SILAC experimental conditions	L/NS + H/TLR3	L/NS + H/TLR3	L/NS + H/TLR3	L/NS + H/NS	L/NS + H/TLR3	L/NS + H/TLR3
Proteins identified[a]	2098	1790	1401	1665	1997	1834
Proteins quantified[b]	1614	1350	1023	1240	1640	1457
Significantly upregulated proteins[c]	98	77	19	8	41	96
Number of MS full scans	387341	405545	408980	427364	411575	325169
Number of MS /MS scan events	128737	126579	168691	116717	128115	337310
Number of MS/MS identified	55184	54350	62702	49135	56786	80472
Peptide sequences identified	16335	13204	10044	11897	14256	12679
Number of SILAC pairs	43017	27730	34729	35473	43336	82196
Number of SILAC pairs sequenced	30353	22226	22662	24138	32952	44882
Number of SILAC pairs identified	16742	13784	12083	14315	19233	17377

Figure 1.

(A) Illustration of the SILAC workflow. **(B)** Summary of samples used and TLR3 pathway state for the SILAC experiment. C1–3: healthy controls; C2NS: healthy control-2 non-stimulated; UNC-93B$^{-/-}$: UNC-93B-deficient patient; P: patient with unknown gene defect. WT: Wild-type HSE: herpes simplex encephalitis. **(C)** Overview of MS results obtained with MaxQuant software.[a] Protein groups identified with protein and peptide FDR = 1%.[b] Protein abundance ratios calculated as median values using a minimum of 3 quantifiable razor peptides.[c] Protein ratios with SigB ≤ 0.05 and SILAC ratios ≥ 1.5. L: light medium; H: heavy medium; NS: non-stimulated cells; TLR3: Poly(I:C) stimulated cells.

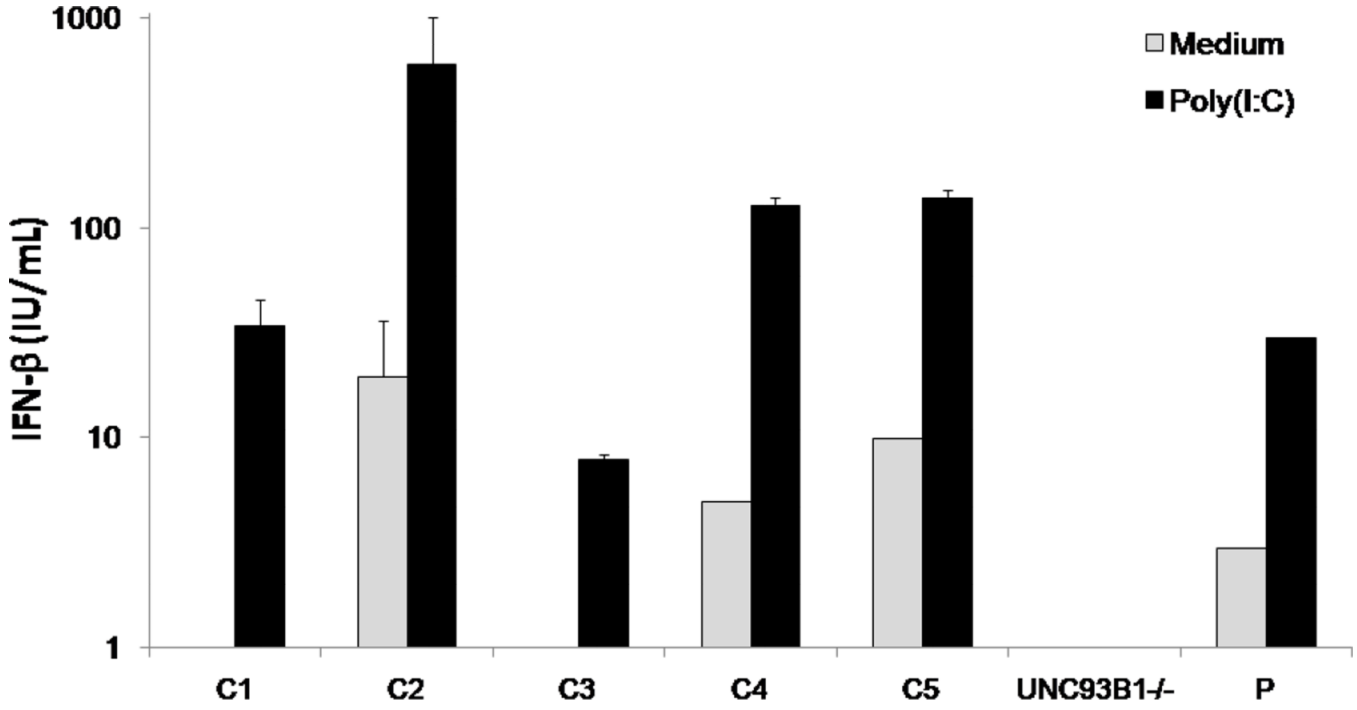

Figure 2.
Production of IFN-β by SV40-fibroblasts after poly(I:C) stimulation for 24 hours as assessed by ELISA. C1–C5: positive healthy controls. UNC93B$^{-/-}$: UNC-93B-deficient patient. Mean values ± SD were calculated from three independent experiments.

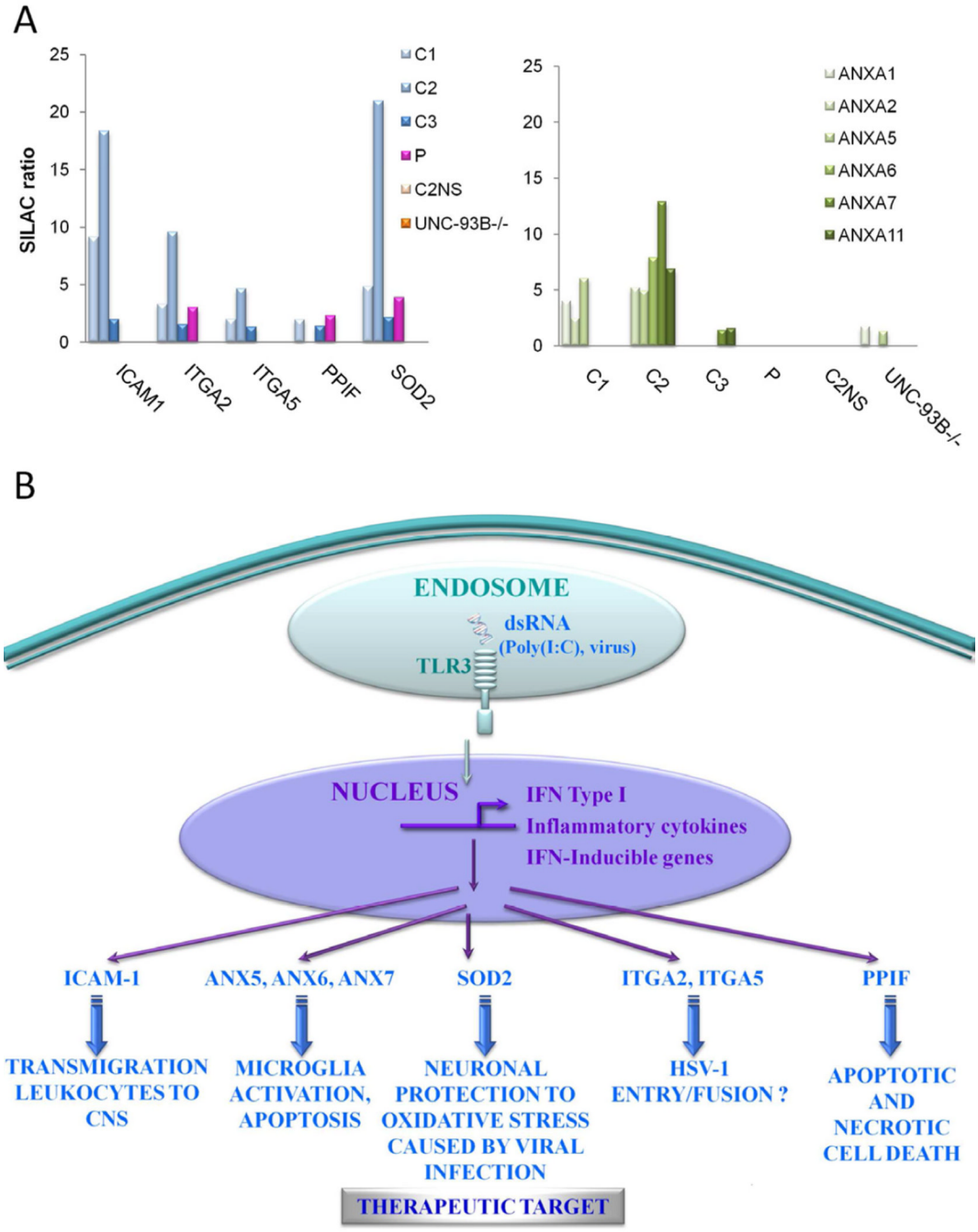

Figure 3.

(A) For proteins with potential biological significance in HSE, the SILAC ratio detected for healthy controls (C1–3), healthy control 2 non-stimulated (C2NS), UNC-93B-deficient patient (UNC-93B$^{-/-}$) and patient with unknown gene defect (P). SigB p-value < 0.05. **(B)** Illustration of potential biological significance in immunity against HSE for proteins up-regulated after TLR3 activation.

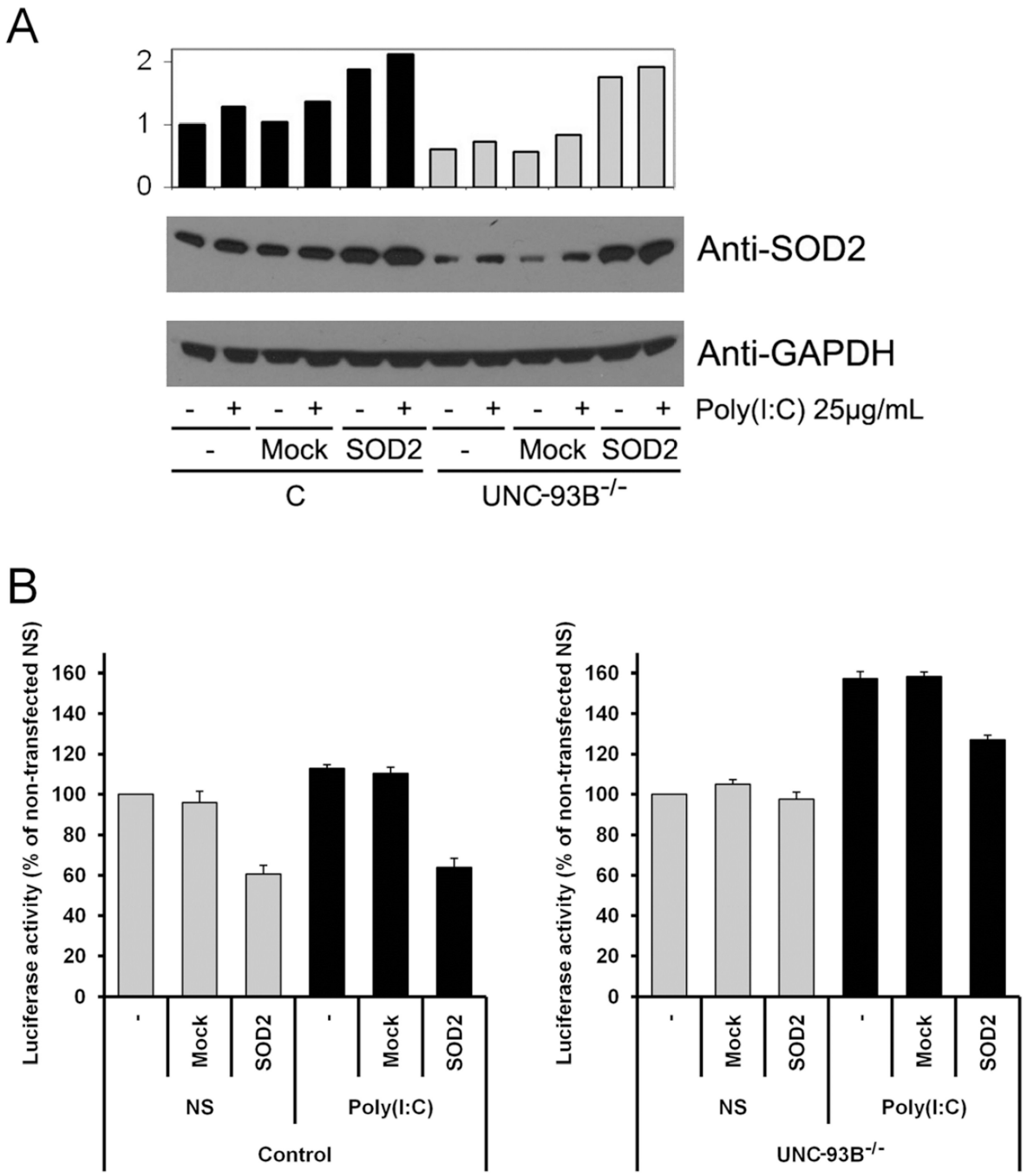

Figure 4.

Human SV40 fibroblast non transfected (−), transfected with SOD2 or Mock vector. **(A)** WB analysis of SOD2 levels. (−): non stimulated; (+): poly(I:C) stimulated. Densitometry normalized with respect to GADPH, expressed as a fold induction over non stimulated/non transfected control cells. The panel is representative of three experiments. **(B)** Caspase-3/7 activity in non stimulated (NS) or poly(I:C) stimulated cells. Luciferase activity represented as percentage,100% is healthy control non stimulated. Mean values ± SD were calculated from three independent experiments. C: healthy control C3; UNC-93B$^{-/-}$: UNC-93B-

deficient patient. Two-sided test were used and a p value less than 0.05 was considered statistically significant.

Table 1

GeneGo pathway maps and process networks with their proteins associated. **(A)** Analysis of the individual data sets for C1–3. **(B)** Enrichment analysis for the union of the C1–3 data sets. Grey panels: pathways/networks known to be implicated in TLR3-IFN signalling. Blue panels: new pathways/networks activated. Threshold: 1.5 (SILAC ratio), SigB p-value < 0.05. Sorting method is statistically significant.

A

C1 SAMPLE		C2 SAMPLE		C3 SAMPLE	
name	**pValue**	**name**	**pValue**	**name**	**pValue**
Ontology: Top GeneGo Pathway Maps		**Ontology: Top GeneGo Pathway Maps**		**Ontology: Top GeneGo Pathway Maps**	
Immune response_Antigen presentation by MHC class I	0,0004167	Immune response_Antiviral actions of Interferons	5,215E-05	Immune response_MIF-mediated glucocorticoid regulation	0,02399
Immune response_IFN alpha/beta signaling pathway	0,007584	Immune response_Antigen presentation by MHC class I	0,0001645	Immune response_IFN alpha/beta signaling pathway	0,02615
Ontology: Top GeneGo Process Networks		**Ontology: Top GeneGo Process Networks**		Immune response_IL-27 signaling pathway	0,02615
Inflammation_Interferon signaling	4,681E-05	Immune response_Antigen presentation	0,0004169	Immune response_Role of integrins in NK cells cytotoxicity	0,04112
Immune response_Phagosome in antigen presentation	0,0006502	Immune response_Phagosome in antigen presentation	0,007849	**Ontology: Top GeneGo Process Networks**	
Immune response_Antigen presentation	0,00111	Inflammation_Interferon signaling	0,01796	Inflammation_Interferon signaling	0,01668
				Immune response_IL-5 signalling	0,0779

B

UNION C1, C2 and C3 SAMPLES

Ontology: Top GeneGo Pathway Maps			Ontology: Top GeneGo Process Networks		
name	**pValue**	**Proteins associated**	**name**	**pValue**	**Proteins associated**
Immune response_IFN alpha/beta signaling pathway	0,007584	ISG54, ISG15, PTP-1B	Inflammation_Interferon signaling	4,68E-05	TAP1, TAP2, ICAM1, ISG15, ISG54, IFI56
Immune response_MIF-mediated glucocorticoid regulation	0,02399	ICAM1	Immune response_Antigen presentation	0,000417	Tapasin, TAP1, TAP2, Calnexin, ICAM1
Immune response_IL-27 signaling pathway	0,02615	ICAM1	Inflammation_NK cell cytotoxicity	0,04988	Histone H1, ICAM1, TfR1, MHC class1
Ontology: Top GeneGo Pathway Maps			**Ontology: Top GeneGo Process Networks**		
name	**pValue**	**Proteins associated**	**name**	**pValue**	**Proteins associated**
Transcription_Role of AP-1 in regulation of cellular metabolism	0,01016	**ITGA2, ITGA5**	Blood coagulation	0,000239	TFPI-2, PLAU, **ITGA2, AnnexinV**

B					
Chemotaxis_CCR4-induced leukocyte adhesion	0,01171	**ICAM1**, Talin	Cell adhesion_Platelet-endothelium-leucocyte interactions	0,000597	**Integrins**, TFPI-2, PAI2, **ICAM1**, PLAU, FGF2
Apoptosis and survival_Endoplasmic reticulum stress response pathway	0,01918	ERP5, **SOD2**	Transcription_mRNA processing	0,01563	hnRNP F, SNRPA, HYPA, KHSRP, SAM68, DDX5, SF3B1, U2AF35
Development_Cross-talk between VEGF and Angiopoietin 1 signaling pathways	0,0283	**ICAM1**	Cell adhesion_Attractive and repulsive receptors	0,02102	**ICAM1, Integrins**, Cortactin
Chemotaxis_Inhibitory action of lipoxins on IL-8- and Leukotriene B4-induced neutrophil migration	0,0319	**ICAM1**, Talin	Proteolysis_Connective tissue degradation	0,03509	TFPI-2, IRAP, PAI2, PLAU
Inhibitory action of Lipoxins on neutrophil migration	0,03911	**SOD2**	Cell adhesion_Cell-matrix interactions	0,05649	**Integrins**
Apoptosis and survival_Anti-apoptotic action of nuclear ESR1 and ESR2	0,04006	**SOD2**	Cell adhesion_Integrin-mediated cell-matrix adhesion	0,05697	**Integrin**, Talin, CD82

Table 2

GeneGo pathway maps and process networks after the analysis of the individual data sets for **(A)** control non-stimulated (C2NS), **(B)** UNC-93B deficient patient cells (UNC-93B$^{-/-}$) and **(C)** HSE patient cells with unknown gene defect (P). Threshold: 1.5 (SILAC ratio), SigB p-value<0.05 and the sorting method is statistically significant.

A		**B**		**C**	
C2NS SAMPLE		**UNC-93B$^{-/-}$ SAMPLE**		**P SAMPLE**	
name	**pValue**	**name**	**pValue**	**name**	**pValue**
Ontology: Top GeneGo Pathway Maps		**Ontology: Top GeneGo Pathway Maps**		**Ontology: Top GeneGo Pathway Maps**	
Cell adhesion_Cadherin-mediated cell adhesion	0,00952	Glycolysis and gluconeogenesis (short map)	1,87E-09	Apoptosis and survival_Granzyme A signaling	0,00097
Development_Slit-Robo signaling	0,01098	Glycolysis and gluconeogenesis p.3 / Human version	6,96E-05	Transcription_P53 signaling pathway	0,0021
Neurophysiological process_EphB receptors in dendritic spine morphogenesis and synaptogenesis	0,0128	Glycolysis and gluconeogenesis p.3	6,96E-05	Transport_Macropinocytosis	0,00271
Cell adhesion_Tight junctions	0,01317	Glycolysis and gluconeogenesis p. 2	0,000152	Transport_RAB3 regulation pathway	0,0037
Transcription_P53 signaling pathway	0,01426	Glycolysis and gluconeogenesis p. 2/ Rodent version	0,000167	Immune response_Antiviral actions of Interferons	0,00479
Neurophysiological process_Receptor-mediated axon growth repulsion	0,01644	Glycolysis and gluconeogenesis p. 2 / Human version	0,000281	Normal wtCFTR traffic / Sorting endosome formation	0,00612
Ontology: Top GeneGo Process Networks		Fructose metabolism	0,001911	DNA damage_NHEJ mechanisms of DSBs repair	0,00681
Transcription_Transcription by RNA polymerase II	0,01626	Fructose metabolism/ Rodent version	0,00276	Delta508-CFTR traffic / Sorting endosome formation in CF	0,00991
Cytoskeleton_Actin filaments	0,01972	Muscle contraction_Delta-type opioid receptor in smooth muscle contraction	0,0035	Immune response_IFN alpha/beta signaling pathway	0,01076
Cell adhesion_Synaptic contact	0,02144	Transcription_Role of Akt in hypoxia induced HIF1 activation	0,003772	Cell adhesion_Endothelial cell contacts by non-junctional mechanisms	0,01076
Reproduction_Spermatogenesis, motility and copulation	0,03227	**Ontology: Top GeneGo Process Networks**		**Ontology: Top GeneGo Process Networks**	
Reproduction_Male sex differentiation	0,03683	Muscle contraction	0,00024	Cytoskeleton_Cytoplasmic microtubules	0,00013
Cytoskeleton_Spindle microtubules	0,1304	Development_Skeletal muscle development	0,00127	Cell cycle_Mitosis	0,00035
Cytoskeleton_Cytoplasmic microtubules	0,1371	Transport_Iron transport	0,004586	Cytoskeleton_Spindle microtubules	0,00068
Development_Neuromuscular junction	0,1732	Protein folding_ER and cytoplasm	0,009973	Inflammation_Interferon signaling	0,00072
Cell adhesion_Cell junctions	0,1881	Cell adhesion_Cell-matrix interactions	0,03411	Cytoskeleton_Macropinocytosis and its regulation	0,00145
Cell adhesion_Attractive and repulsive receptors	0,2018	Cell adhesion_Integrin-mediated cell-matrix adhesion	0,03452	Cell adhesion_Integrin-mediated cell-matrix adhesion	0,00498
		Immune response_Phagocytosis	0,03703	Translation_Translation initiation	0,00665

A	B		C	
	Development_Blood vessel morphogenesis	0,04052	Cytoskeleton_Actin filaments	0,00762
	Cell adhesion_Attractive and repulsive receptors	0,1177	Translation_Elongation-Termination	0,00786
	Signal transduction_Insulin signaling	0,1177	Cytoskeleton_Intermediate filaments	0,00823